Unsupervised multi-tissue decomposition of single-shell diffusion-weighted imaging by generalization to multi-modal data

Daan Christiaens[1,2], Frederik Maes[1,2], Stefan Sunaert[2,3], and Paul Suetens[1,2,4]

[1]ESAT/PSI, Department of Electrical Engineering, KU Leuven, Leuven, Belgium, [2]Medical Imaging Research Center, UZ Leuven, Leuven, Belgium, [3]Translational MRI, Department of Imaging & Pathology, KU Leuven, Leuven, Belgium, [4]Medical IT Department, iMinds, Leuven, Belgium

Introduction

In recent years, data-driven analysis of diffusion-weighted imaging (DWI) has been extended beyond white matter (WM), explicitly modelling partial voluming with adjacent tissues. *Supervised* methods such as single- and multi-tissue constrained spherical deconvolution (CSD)[1,2] reconstruct orientation distribution functions (ODF) of WM, grey matter (GM), and cerebrospinal fluid (CSF), given response functions (RF) for these tissues. These RFs are calibrated to the data based on prior segmentations, either obtained from T_1-weighted anatomical data2 or directly from DWI[3,4]. Alternatively, *unsupervised* methods decompose DWI data in tissue components, akin to blind source separation, jointly optimizing tissue RFs and ODFs based on sparsity or convexity constraints[5,6].

However, the number of tissue classes is inherently limited by the number of shells (b-values) in the data. The 3-tissue model that was found optimal for healthy human brain data[6] thus requires multi-shell data. Yet, in many cases only "single-shell" (b=0 and b=X) data is available. This study augments unsupervised tissue decomposition with multi-modal data. Specifically, we include a T_1-weighted image (T1) in the framework of convexity-constrained non-negative spherical factorization (CNSF)[6] and illustrate its applicability for decomposing single-shell DWI into WM, GM and CSF.

Method

The linear multi-tissue model decomposes the DWI signal into separate tissues, each characterized by a global, axially symmetric response function, and represents the tissue contribution in a voxel as the spherical convolution of its RF with a non-negative ODF. By casting all functions to the spherical harmonics basis, the convolution reduces to a tensor multiplication. If the RFs are unknown, this translates into a non-negative factorization problem[5,6]. Because this problem is underdetermined, CNSF additionally imposes that all RFs are convex combinations of the measured signal after reorientation[6].

Multi-modal data is incorporated in the decomposition as additional isotropic channels, akin to the b=0, under the same assumption of linear partial voluming. As such, the estimated tissue RFs will include the expected T1-intensity. The tissue ODFs remain unchanged, and characterize both density (integral across the sphere) and directional structure. In all experiments, shell weights are set to their respective number of DWI volumes. The T1 is arbitrarily assigned a weight corresponding to 100 DWI volumes.

Results

Dataset 1 is provided by the human connectome project[7]. Dataset 2 is acquired on a Philips Achieva 3T, isotropic voxel size 2.5mm, 10;25;40;75 gradient directions at b=0;700;1000;2800s/mm^2 respectively, corrected for distortion using reverse-phase encoding, and for field inhomogeneity. The T1 is assumed to be registered and subsampled to the DWI.

First, we compare unsupervised tissue decomposition of multi-shell DWI with and without including T1. The RFs, shown in the top and middle rows of Fig. 1, are similar and correspond well with the ground-truth RFs, estimated with a supervised method[2]. Figure 2 shows the ODFs of the estimated tissue components. In both cases, the anisotropic component is associated with WM, two isotropic components are associated with GM and CSF. When including T1, the WM fraction is more sharply delineated, while GM becomes slightly fuzzier. In the ventricles, the CSF component is sensitive to Gibbs-ringing artefacts in the T1.

Secondly, we evaluate 3-tissue decomposition in single-shell DWI, augmented with T1. The RFs are plotted in Fig. 1, bottom row. Figure 3 shows the reconstructed ODFs in different shells, compared to single-shell CSD[1]. WM, GM, and CSF are effectively separated, even at low b-values. Close-ups of the WM ODF, reconstructed from b=2800s/mm^2, are shown in Fig. 4, and indicate improved handling of partial voluming w.r.t. single-shell CSD, akin to multi-tissue CSD and CNSF.

Discussion

Our results show that augmenting single-shell DWI with T1 provides the necessary contrast to discriminate three tissue components, associated with WM, GM, and CSF. While related work has used a T1-segmentation to adapt the CSD response function locally[8], our approach instead finds a set of tissue RFs that explain the data (DWI and T1), without requiring prior segmentation. The comparison with single-shell CSD in Fig. 3 shows that even at low b-values, where CSF signal yields large fibre ODFs in the ventricles, our method is able to reconstruct fibre ODFs with no observable CSF contamination. Similarly, Fig. 4 illustrates that the multi-tissue decomposition accounts for partial voluming, and ultimately benefits ODF reconstruction and subsequent tractography[2,3].

The extension to multi-modal data is not only applicable to T1, but also to FLAIR, MRS metabolite concentration, or any other contrast that supports the assumption of linear partial voluming. Future work could investigate its use for studying tissue structure in pathology.

Conclusion

We generalized CNSF for combined analysis of DWI and other modalities, and exemplified its use with 3-tissue decomposition of single-shell DWI in combination with T1.

Acknowledgements

D.C. is supported by Ph.D. grant SB 121013 of the Agency for Innovation by Science and Technology (IWT). Data were provided in

part by the Human Connectome Project, WU-Minn Consortium (Principal Investigators: David Van Essen and Kamil Ugurbil; 1U54MH091657) funded by the 16 NIH Institutes and Centers that support the NIH Blueprint for Neuroscience Research; and by the McDonnell Center for Systems Neuroscience at Washington University.

References

1. Tournier J-D, Calamante F, Connelly A. Robust determination of the fibre orientation distribution in diffusion MRI: Non-negativity constrained super-resolved spherical deconvolution. NeuroImage 35(4):1459–1472 (2007).
2. Jeurissen B, Tournier J-D, Dhollander T, Connelly A, Sijbers J. Multi-tissue constrained spherical deconvolution for improved analysis of multi-shell diffusion MRI data. NeuroImage 103:411–426 (2014).
3. Christiaens D, Reisert M, Dhollander T, Sunaert S, Suetens P, Maes F. Global tractography of multi-shell diffusion-weighted imaging data using a multi-tissue model. NeuroImage 123:89–101 (2015).
4. Jeurissen B, Tournier J-D, Sijbers J. Tissue-type segmentation using non-negative matrix factorization of multi-shell diffusion-weighted MRI images. Proceedings of ISMRM 23:349 (2015).
5. Reisert M, Skibbe H, Kiselev V. The diffusion dictionary in the human brain is short: Rotational invariant learning of basis functions. Proceedings of Computational Diffusion MRI and Brain Connectivity. Mathematics and Visualisation 47–55 (2014).
6. Christiaens D, Maes F, Sunaert S, Suetens P. Convex non-negative spherical factorization of multi-shell diffusion-weighted images. Proceedings of MICCAI 2015. Lecture Notes in Computer Science 9349:166–173 (2015).
7. Van Essen D, Smith S, Barch D, Behrens T, Yacoub E, Ugurbil K. The WU-Minn human connectome project: an overview. NeuroImage 80:62–79 (2013).
8. Roine T, Jeurissen B, Perrone D, Aelterman J, Philips W, Leemans A, Sijbers J. Informed constrained spherical deconvolution. Medical Image Analysis 24(1):269–281 (2015).

Figures

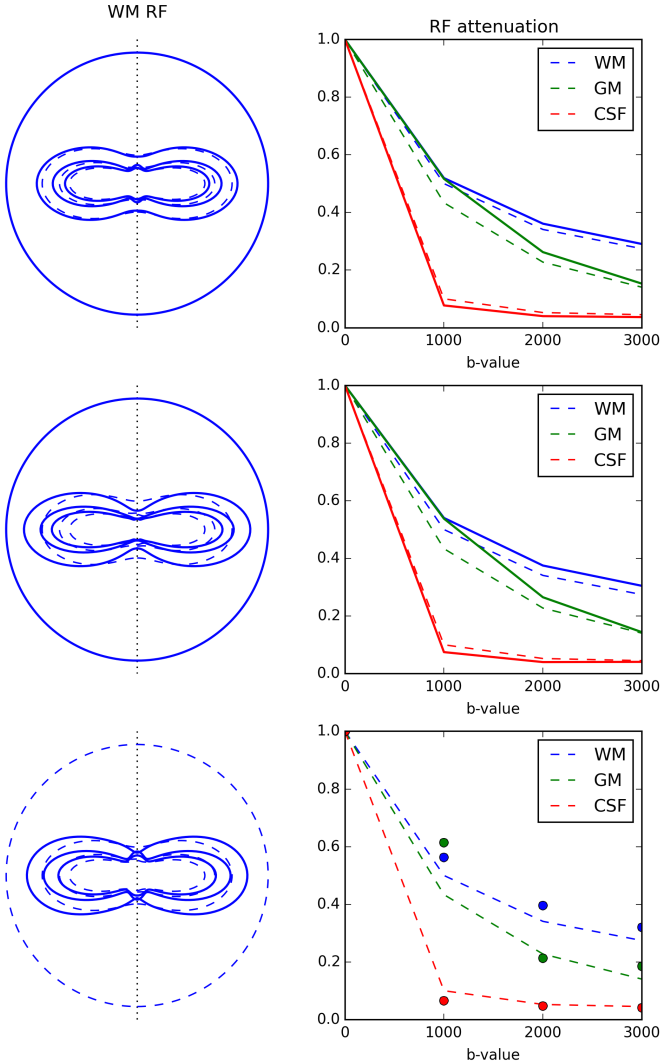

Fig. 1: Response functions estimated with CNSF in dataset 1, compared to ground truth (dashed lines). Top: multi-shell DWI. Middle: multi-shell DWI + T1 anatomical image. Bottom: single-shell DWI + T1, for each shell separately.

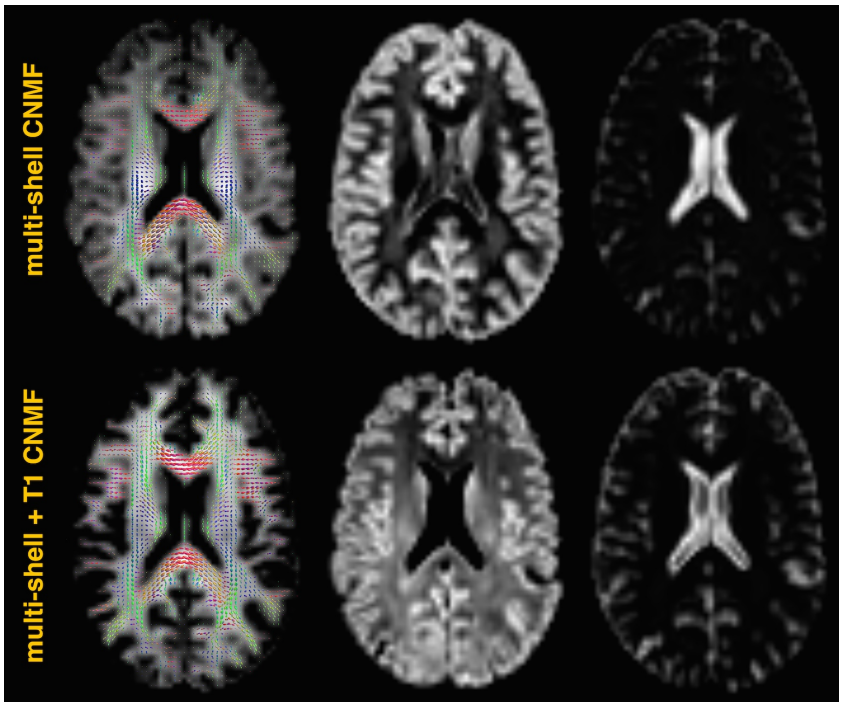

Fig. 2: Comparison between CNSF of multi-shell DWI with and without T1 anatomical data in dataset 2.

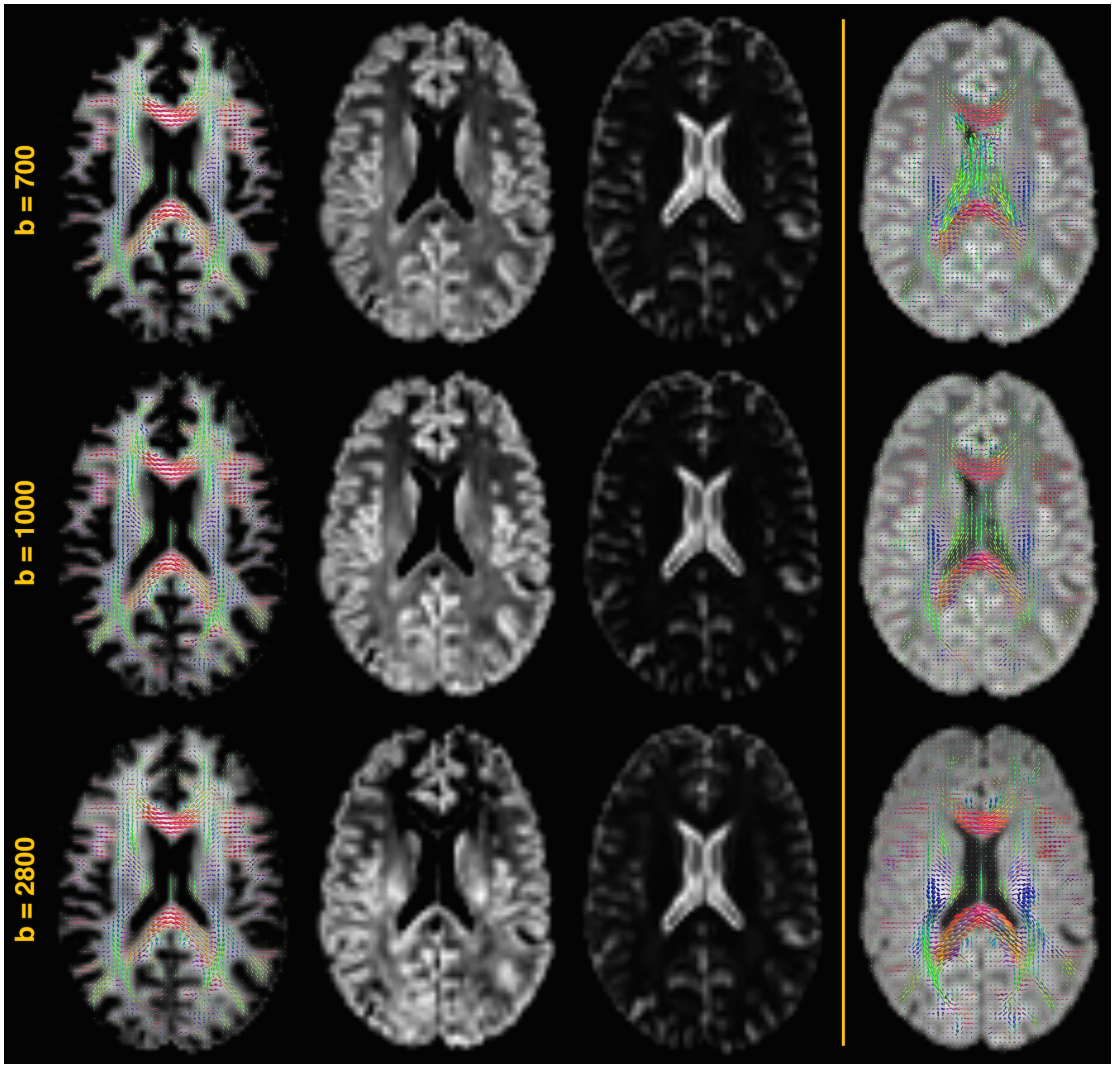

Fig. 3: Left: Tissue ODFs estimated from T1 and single-shell DWI in dataset 2, estimated with CNSF. Right: Fibre ODF of single-shell CSD.

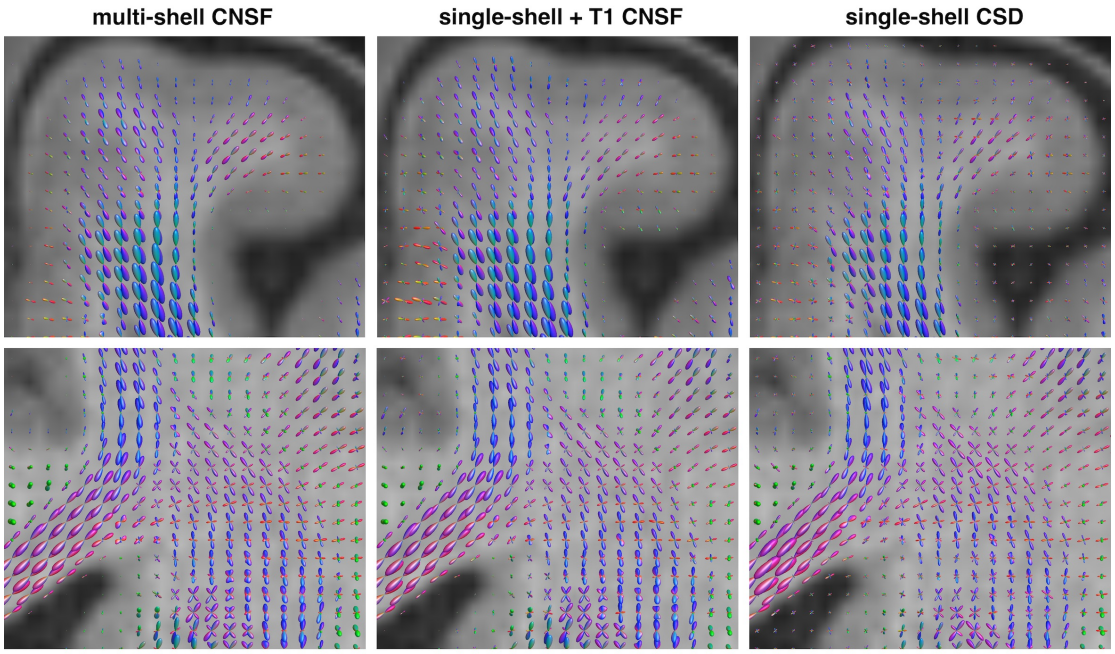

Fig. 4: Comparison of the proposed method to multi-shell CNSF and single-shell CSD in dataset 1. Coronal slice of the left frontal superior gyrus (top) and the semioval centre (bottom), overlaid on the T1-image.